Liquid Crystals
Publication details, including instructions for authors and subscription information:
http://www.informaworld.com/smpp/title~content=t713926090

Electro-optic properties of liquid crystal phase gratings and their simulation using a homogeneous alignment model

Hideya Murai[a]
[a] NEC corporation, Functional Devices Research Laboratories 4-1-1, Kanagawa, Japan

To cite this Article Murai, Hideya(1993) 'Electro-optic properties of liquid crystal phase gratings and their simulation using a homogeneous alignment model', Liquid Crystals, 15: 5, 627 — 642
To link to this Article: DOI: 10.1080/02678299308036482
URL: http://dx.doi.org/10.1080/02678299308036482

LIQUID CRYSTALS, 1993, VOL. 15, NO. 5, 627–642

Electro-optic properties of liquid crystal phase gratings and their simulation using a homogeneous alignment model

by HIDEYA MURAI
NEC corporation, Functional Devices Research Laboratories 4-1-1, Miyazaki, Miyamae-ku, Kawasaki, Kanagawa 216, Japan

(*Received 23 November 1992; accepted 25 April 1993*)

Electro-optic properties of liquid crystal phase gratings (LCPGs), regarding groove depth, temperature and a cell gap, have been studied. The off response times are proportional to the square of the groove depth. The transmitted light colour depends on temperature. When there is a gap between the grating and the opposite substrate, their transmittance–voltage curve has a maximum and a minimum. The authors have also simulated the LCPG properties using a homogeneous alignment model. The simulating results coincide with experimental results; therefore the simulation method is considered useful to predict LCPG properties.

1. Introduction

Several types of liquid crystal devices were proposed as colour displays without colour filters. A liquid crystal phase grating (LCPG) is one such device which consists of a liquid crystal and a phase grating [1]. In a previous paper [2], the authors reported the possibility of using liquid crystal phase gratings as colour projection devices. Their response times are less than 10 ms, much shorter than those for the twisted nematic mode. The transmitted light colour can be regulated by less than 10 V. Red, green, blue and white have been obtained. The LCPG can also be operated with unpolarized light, when two of the LCPGs are combined perpendicularly.

Other important properties of the LCPG, regarding groove depth and temperature dependence, have not yet been reported. The effect of a grating–substrate gap, which has a peculiar effect on the LCPG properties, has also not been investigated. Furthermore, it is important to connect the LCPG properties with the properties of the liquid crystal and the grating material, because this demonstrates a good way to improve the LCPG properties.

In this paper, the authors report results obtained through investigating the influence on LCPG properties of groove depth of the phase grating, temperature and the existence of a gap between the phase grating and the opposite substrate. The authors have also simulated the LCPG from the properties of the liquid crystal and the grating material using a homogeneous alignment model. In this way, they have found that the simulation method is a useful way to predict the LCPG properties.

2. LCPG structure and mechanism

The structure of a LCPG is shown in figure 1. The LCPG consists of a square wave type phase grating, and a liquid crystal, which covers the grating grooves. They are held between two substrates with a transparent electrode. Optical lengths for the phase grating part and the liquid crystal part (=the grating groove part) depend on the

0267-8292/93 $10·00

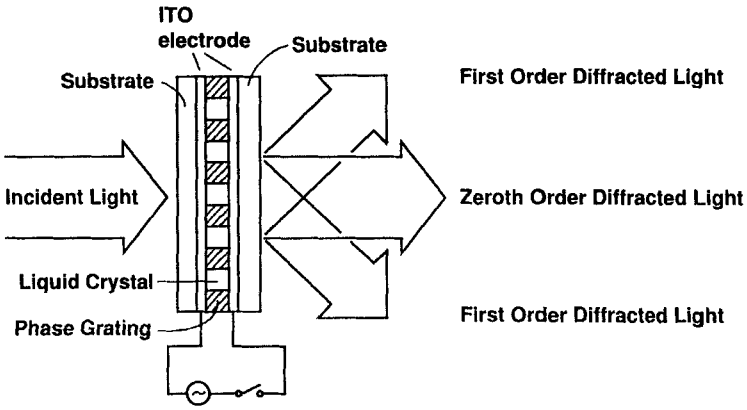

Figure 1. Structure of a liquid crystal phase grating.

refractive indices of the grating material and the liquid crystal, respectively. The refractive index of the liquid crystal depends on the direction of the liquid crystal director. The director is regulated by the applied voltage.

Incident light passes through the LCPG when there is no phase shift between the two parts. When there is some phase shift, incident light is decreased and bent. When absorption and reflection in the LCPG are ignored, zeroth order efficiency (=transmittance) is shown by

$$T(\lambda)=\cos^2(\pi\Delta nd/\lambda), \tag{1}$$

where λ is wavelength, Δn is the refractive index difference between the grating material and liquid crystal and d is grating depth [3].

When white light is incident perpendicularly to the LCPG, some light wavelengths pass through the LCPG, the other light wavelengths being bent by the LCPG. Therefore, by eliminating the bent light using a slit, the LCPG works as a colour device.

3. Experimental

Square wave phase gratings for the LCPGs were prepared using a deep UV lithography technique, as described in the previous paper [2]. Poly(methyl methacrylate) (PMMA) (Du Pont, Elvacite 2041) was used as the grating material, since its refractive index is nearly equal to the ordinary refractive index of the liquid crystal. The refractive index of PMMA is 1·492 at 589 nm [4]. The PMMA was dissolved in 1-acetoxy-2-ethoxyethane (10 wt%) and coated onto glass plates. 1·0–2·5 μm PMMA layers were obtained. After exposing to deep UV light and developing with mixed solvents, 5 μm/5 μm line and space pattern phase gratings were obtained.

An ITO-glass plate, the surface of which was coated with polyimide, was used as an opposite substrate. Except for experiments studying the cell gap, the ITO-glass plate was fixed on the phase grating without spacers. Then, the plateau part of the grating was in contact with an opposite substrate. The grating line direction was parallel to the rubbing direction for the polyimide alignment layer.

The liquid crystal used in these experiments was a commercially available liquid crystal mixture E7 and E8, manufactured by Merck Ltd, England. Their dielectric constants and refractive indices are shown in the table. The liquid crystal penetrated the groove part of the grating by capillary action.

Properties of the liquid crystal and grating material for the calculations.

		E7 [5]	E8 [5]	PMMA [4]
Refractive index (589 nm, 20°C)	n_e	1·746	1·771	—
	n_o	1·522	1·525	1·492
Dielectric constant (1 kHz, 20°C)		13·8	15·6	—

Electro-optic properties, which depend on light wavelength, were measured with a spectrophotometer (Otsuka Electronics, LCD-5000). A slit was used to separate zeroth order diffracted light from light of other orders. A polarizer was placed between the light source and the LCPG cell in all measurements. The polarized plane for the light was parallel to the grating lines.

Response times were measured using a He–Ne laser (NEC GLG5321) and a photodiode connected to a storage oscilloscope (LeCroy 9400A). No polarizer was used in this experiment, since the He–Ne laser light was linearly polarized. The on time was defined as the time needed for the change in transmittance from 0 per cent at time zero to 90 per cent of its maximum value. The off time was defined as the time needed for the change in transmittance from 100 per cent at time zero to 10 per cent of its maximum value.

Signals applied in the measurements were 1 kHz square wave AC. All electro-optic properties (except temperature dependence) were measured at 25°C.

4. Results and discussion

4.1. *Effect of grating groove depth*

As shown in the previous paper [2], grating groove depth of the LCPG affects the transmitted light colour. The grating depth not only affected transmitted light colour, but also response time. In order to compare the response times under the same conditions, appropriate light wavelengths were selected for each LCPG. Under this condition, transmittance increased monotonically with increased voltage application.

Figure 2 shows the dependence of the response times on the applied voltage. For each LCPG depth, the on times are inversely proportional to the square of the applied voltage. On the other hand, the off times are slightly increased with applied voltage. Similar voltage dependences of response time were reported for the dynamic scattering mode and the twisted nematic mode [6].

It is known that the response times for the twisted nematic mode and homogeneous mode are proportional to the square of the cell thickness [7]. The off times for the LCPGs are plotted against the square of groove depth in figure 3. The off time is proportional to the square of the grating depth, i.e. the liquid crystal layer thickness. The result that the response time dependence for the LCPG is the same as that for a homogeneous cell means that the effect of the grating groove side walls is small in these experiments.

4.2. *Temperature dependence of transmitted light colour*

The properties of liquid crystal materials change with temperature. Anisotropy of the refractive indices, elastic constants and viscosity decrease as the temperature rises. Although the extent is smaller than those for the liquid crystal, the refractive index of the grating material also changes. Therefore, the LCPG properties change with changing temperature.

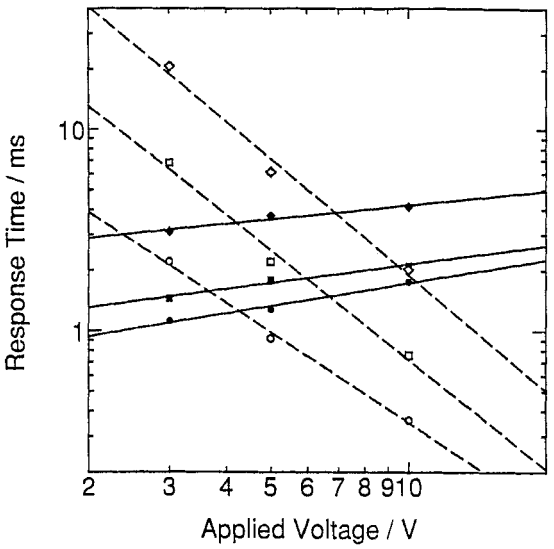

Figure 2. Dependence of response times on the applied voltage. τ_{ON}, (○), 0·9 μm, (□), 1·0 μm, (◇), 1·4 μm. τ_{OFF}, (●), 0·9 μm, (■), 1·0 μm, (◆), 1·4 μm. The liquid crystal was E7, and the applied frequency was 1 kHz.

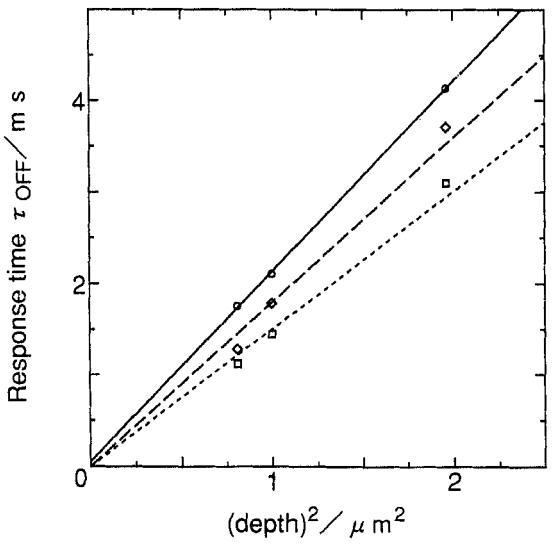

Figure 3. Dependence of the off time on the grating depth. The applied voltages were (○), 10 V, (□), 5 V, and (◇), 3 V, at 1 kHz the liquid crystal was E7.

The temperature dependence of the transmitted light spectra with no applied voltage is shown in figure 4. The LCPG groove depth is 2·3 μm. As the temperature rises, the peak wavelengths shift to a short wavelength. The changes in the peak wavelength with changing temperature are smaller for a short wavelength region than for a long wavelength region. This result can be explained, considering the fact that the changes in the refractive indices are smaller in the short wavelength region. The change in the spectra can be calculated from the index change, using a homogeneous alignment model, as shown in § 5.4.

Change in the transmittance light colour under applied voltage are shown on the colour charts in figure 5. As the temperature rises, the same colour appears with a lower applied voltage.

4.3. *Cell gap effect*

The results mentioned previously were obtained when the phase gratings are in contact with both substrates. When there is a gap between the phase grating and the substrate, as shown in figure 6, different results may be obtained.

An LCPG cell which has a gap between the phase grating and the opposite electrode was made. The cell had a 1·4 μm grating depth and a 2·8 μm gap. The LCPG has minimum transmittance at 630 nm under no applied voltage. Figure 7 shows the transmittance dependence on applied voltage for the LCPG. The light wavelength used in this measurement was 630 nm. When the phase gratings are in contact with the opposite electrode, their transmittance changes monotonically as reported previously [2]. On the other hand, when there is a gap between the grating and the opposite electrode, maximum and minimum values appear in the transmittance–voltage curve. The initial gradient of the curve is larger than that when there is no gap in the LCPG.

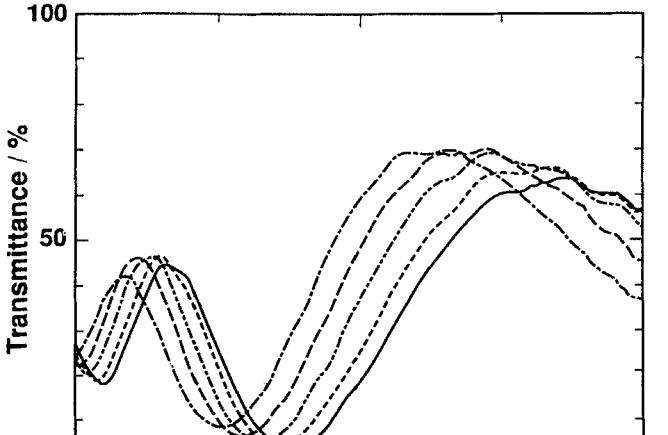

Figure 4. Dependence of the transmitted light spectra on temperature without voltage application. (——), 10°C; (- - - -), 20°C; (— · — · —), 30°C; (— — —), 40°C; (— - — - —), 50°C. The liquid crystal was E8 and the grating depth was 2·3 μm.

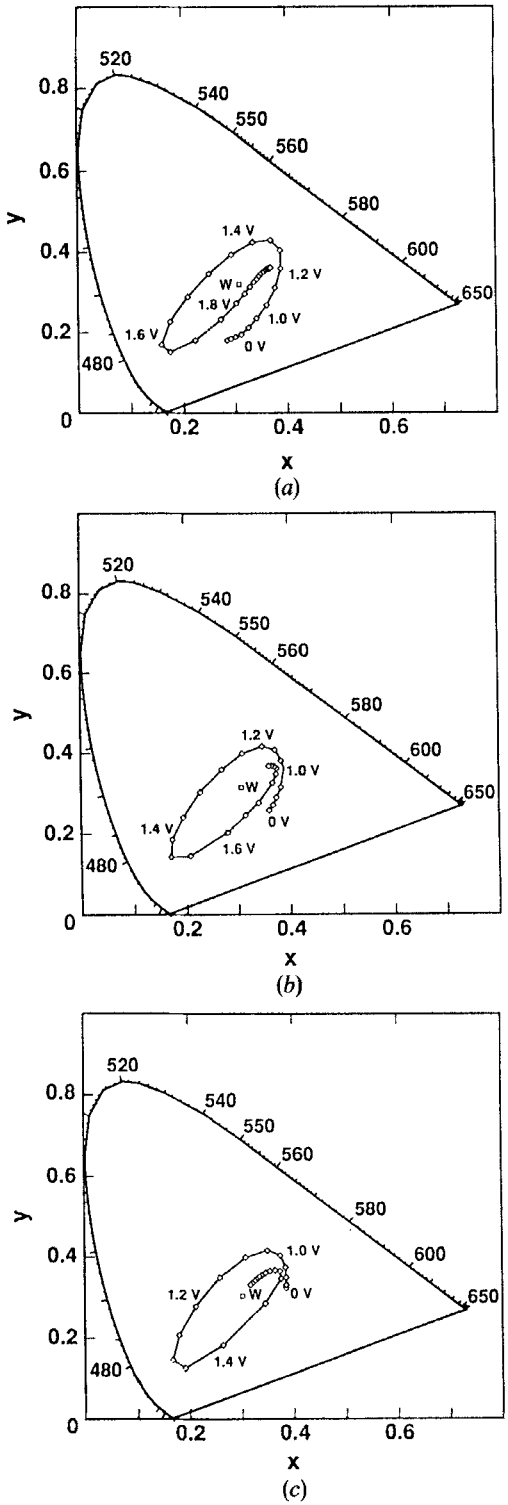

Figure 5. Change in the transmitted light colour with temperature. The liquid crystal was E8, and the grating depth was 2·3 μm (*a*) 10°C, (*b*) 30°C and (*c*) 40°C.

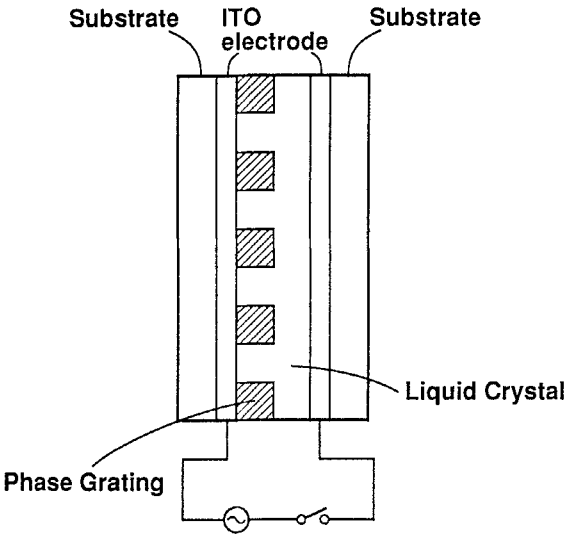

Figure 6. Structure of a PDLC with a gap between the convex part of gratings and opposite electrode.

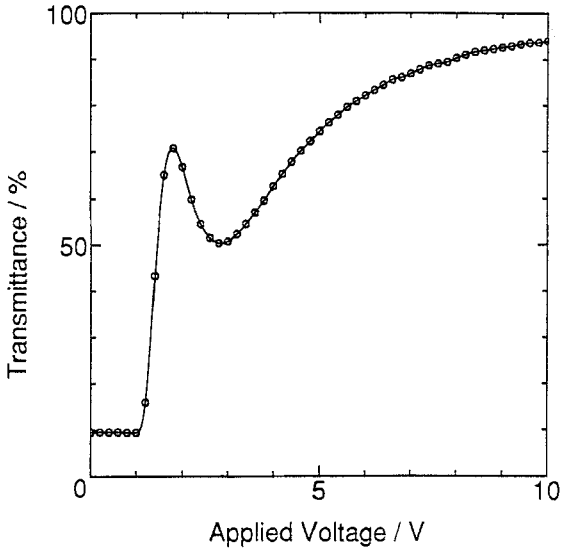

Figure 7. Dependence of transmittance on the applied voltage for a LCPG gap. 2·8 μm, and grating depth of 1·4 μm. The liquid crystal was E8, and the measurement wavelength was 630 nm.

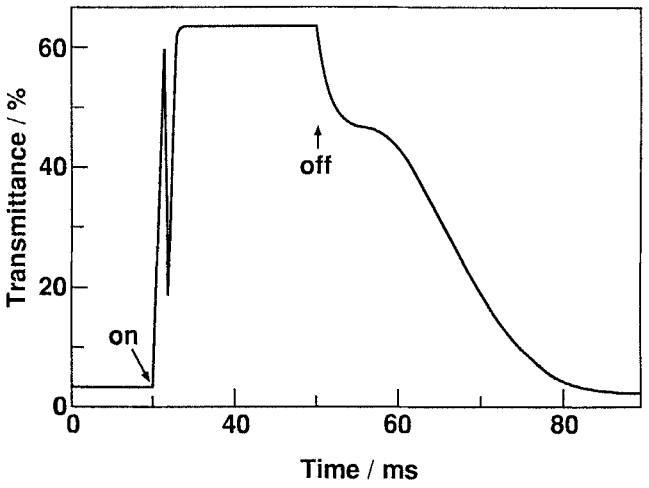

Figure 8. Transmittance change in a gap LCPG when the voltage turns on and off. The gap was 2·8 μm, and the grating depth 1·4 μm. The liquid crystal was E8, and the measurement wavelength was 630 nm. $\tau_{off} = 50$ ms.

The origins for these results are in the liquid crystal existing in the gap and increasing the layer thickness of the liquid crystal. These factors are explained by two liquid crystal parts, which have different thicknesses in a homogeneous alignment model, as shown in § 5.5.

Figure 8 shows the transmittance change when the applied voltage is turned on and off. This curve is not as simple as that for a no-gap LCPG [2]. Decay time is about 50 ms, which is much larger than that for a no-gap 1·4 μm LCPG (see figure 4). This result can be accounted for by the liquid crystal layer thickness being increased by the gap.

5. Simulation of transmittance

5.1. *Simulation model*

In order to make a LCPG, several steps are needed and they are not easy. If the LCPG properties could be estimated only from properties of the liquid crystal and the phase grating material, it would become a very useful way to design LCPGs. In this section, the authors propose an LCPG model, in which the liquid crystal aligns homogeneously. In this model, the LCPG transmittance is calculated from properties of the liquid crystal, i.e. the refractive indices, the dielectric constant, the elastic constant, the viscosity, and the refractive index of the grating material.

The model used in the authors' simulation is shown in figure 9. The liquid crystal layer in the LCPG is regarded as consisting of two parts, i.e. the plateau part and the groove part of the phase grating. When the plateau part of the grating is in contact with the opposite electrode, the liquid crystal layer of the plateau part disappears. The effect of the grating side wall is not considered in this model. This assumption may be reasonable, when the groove width of the grating is much larger than the groove depth. In the authors' simulation, it was also assumed that the liquid crystal was strongly anchored on the substrate. In the previous paper [2], homogeneous alignment of the liquid crystal had been confirmed when no voltage was applied. However, the anchoring strength between the substrate and the liquid crystal is not known. There is a

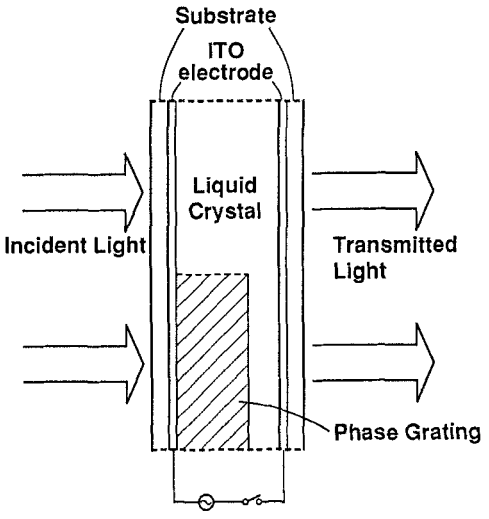

Figure 9. Homogeneous alignment model for the LCPG.

rubbed polyimide layer on the opposite substrate; then this assumption may be correct for the substrate. On the other hand, there is no alignment layer and rubbing on the grating substrate, therefore the assumption is not necessarily correct for the experiments.

Several properties of the grating material and the liquid crystal determine the LCPG properties. The phase grating is a solid material, so only its refractive index affects the LCPG properties and the extent of the effect is small. On the other hand, the liquid crystal affects the LCPG properties, not only through the refractive index but also through the dielectric constant, the elastic constant and the viscosity. The dependence of those properties on wavelength and temperature is large.

The authors' simulation method is as follows. It is difficult to calculate the tilt angle of the liquid crystal analytically, because the dielectric constant of the liquid crystal is a function of the tilt angle, and the electric field in the liquid crystal layer is also changed [8, 9]. Therefore, the authors numerically calculated the tilt angle between the molecular axis of the liquid crystal and the substrate. The commercially available liquid crystal simulator 'DIMOS' [10] was used to calculate the tilt angle. Transmitted light (zeroth order diffraction) intensities of the LCPGs are a function of the optical length. The optical difference between the plateau part and the groove part of the liquid crystal layer can be calculated from these results, using the following equation:

$$D = D(\text{groove}) - D(\text{plateau}) \tag{2}$$

$$= \int n_{LC} dx - \left(\int n_{LC} dx + n_g \times d \right), \tag{3}$$

where the D values are optical lengths and n_{LC} and n_g are the refractive indices of the liquid crystal and the grating material, respectively. The grating groove depth is d. The equations are integrated over the LCPG cell thickness. When polarized light is used and its polarized plane is parallel to the direction of liquid crystal alignment, the liquid crystal refractive index is given as,

$$n_{LC} = n_e \times n_o / (n_e^2 \times \cos^2 \theta + n_o^2 \times \sin^2 \theta)^{1/2} \tag{4}$$

where θ is tilt angle, and n_e and n_o are the extraordinary and ordinary refractive indices of the liquid crystal, respectively. The physical properties of liquid crystals E7 and E8, and the grating material (PMMA), used in the simulation are shown in the table.

5.2. *Transmittance*

Figure 10 shows a comparison between the measured and simulated LCPG spectra. The spectra are shown for three grating depths without voltage application. The shape and the wavelength in which the transmittance has a maximum or minimum value coincide well. Absolute values of the transmittance are not coincident. One reason for

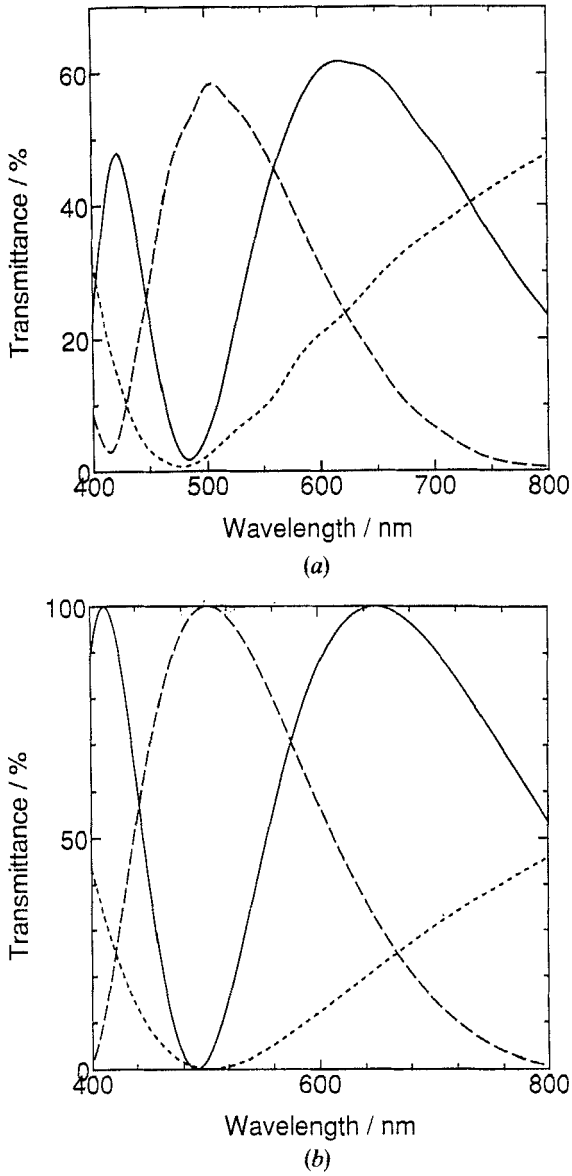

Figure 10. Comparison of LCPG spectra with no applied voltage, for (*a*) measured, (*b*) calculated. Grating depth: (- - - -), 0·9 μm; (- - —), 1·8 μm; (——), 2·2 μm. The liquid crystal was E7.

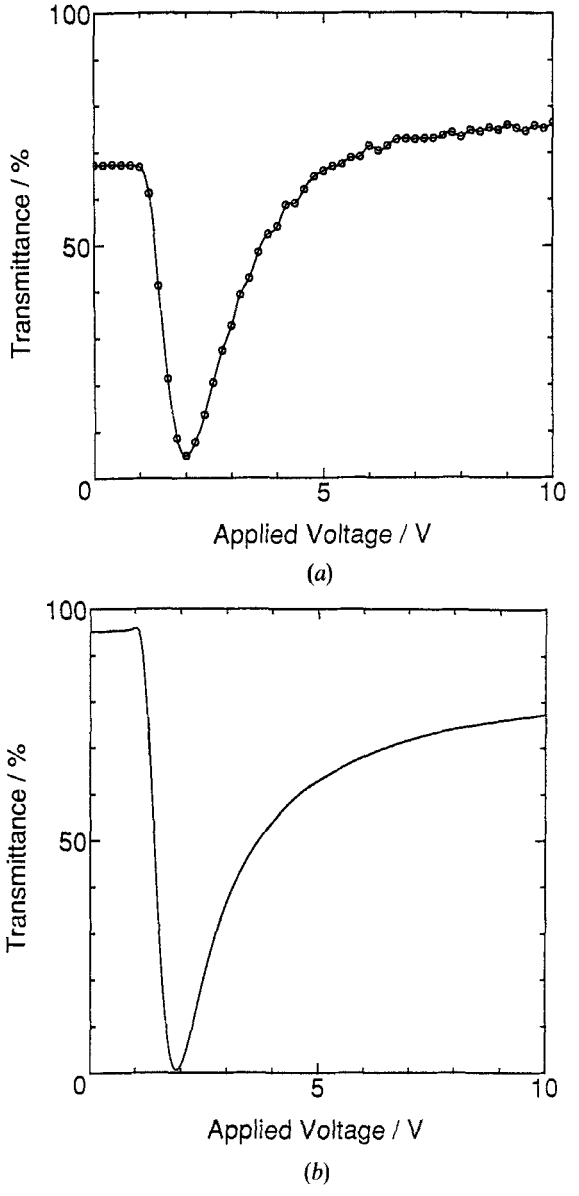

Figure 11. Transmittance–voltage curve, for (*a*) measured, (*b*) calculated. The grating depth was 2·2 μm, the wavelength 550 nm, and the liquid crystal E7.

this result is that absorption in individual layers and reflection at the interface are not considered in the authors' simulation. Another reason is that the grating shape is not strictly rectangular, as shown in the previous paper [2]. The transmittance decreases when the grating shape is not strictly rectangular.

Transmittance of a LCPG changes with voltage application as shown in figure 11. The grating depth was 2·2 μm. The wavelength used for the measurements was 550 nm. The measured and calculated transmittance values are closely coincident, except for the absolute transmittance value. The reason for the inconsistency is similar to that in figure 10.

5.3. *Response time*

Changes in the LCPG transmittance, after removing the applied voltage (2 V), are shown in figure 12. The grating depth was 2·2 μm. The liquid crystal used was E7. Its rotational viscosity [11] was used as a liquid crystal viscosity in the simulation. The shapes of the transmittance–time curves are almost the same and the off times are nearly equal. The calculated transmittance has a small peak at about 7 ms. This result stems from the fact that the transmittance maximum as a function of the wavelength is

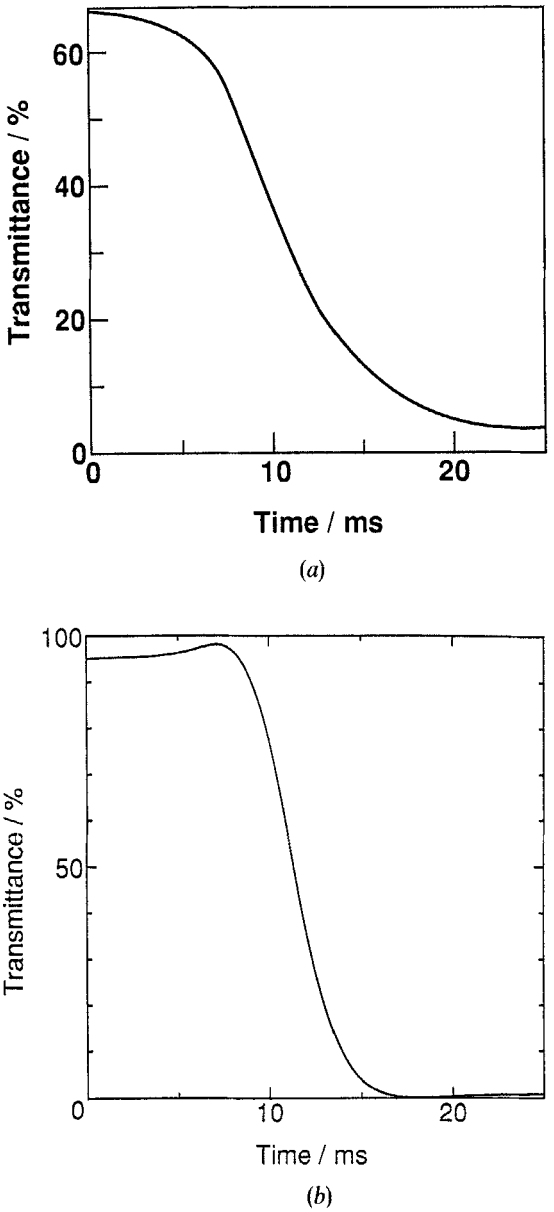

Figure 12. Comparison of the transmittance change after removing the applied voltage. (*a*) Measured, (*b*) calculated. The applied voltage was 2 V, the liquid crystal E7, the grating depth 2·2 μm, and the wavelength was 550 nm.

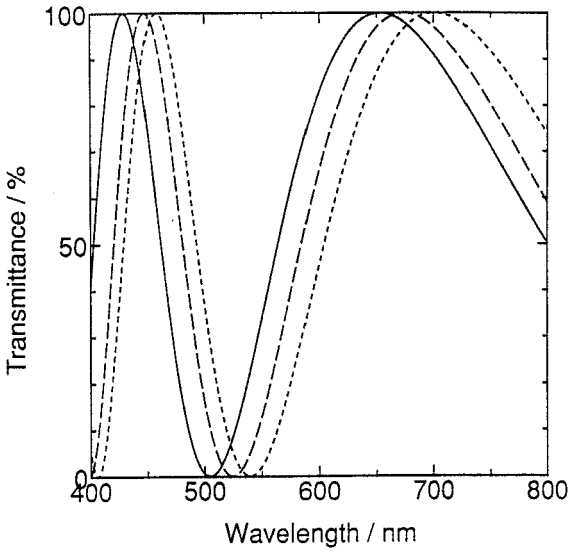

Figure 13. Simulation of the temperature dependence of transmittance. Temperature: (----), 20°C; (– – –), 30°C; (——), 40°C. The liquid crystal was E8, and the grating depth was 2·2 μm.

not strictly the same as that measured. The calculated transmittance change is a little steeper and occurs slightly faster than the measured one. This difference perhaps comes from restriction in the liquid crystal and the fact that the grating side walls surface is not considered in the calculation.

5.4. *Temperature dependence*

Dependence of the transmitted light spectrum on temperature can also be calculated in the model. The refractive index of liquid crystal E8 and the grating material (PMMA) were measured as a function of wavelength and temperature. Simulation results for the temperature dependence of the spectra are shown in figure 13. These results are for when no voltage is applied. The coincidence of the maximum and minimum wavelengths between the calculated and experimental values (figure 4) is fairly good. Absolute values of the transmittance are not coincident. The reason is similar to that given in § 5.2.

5.5. *Gap effect*

When there is a gap between the phase grating and the opposite electrode, the transmittance–voltage curve has maximum and minimum values, as shown in figure 7. This result can be explained by differences in the liquid crystal layer thickness in the plateau part and the groove part of the phase grating. However, when only the liquid crystal thickness is different, this result does not appear. The tilt angles of the liquid crystal molecules in the centre of the liquid crystal layers, which had different thicknesses were calculated and are plotted against applied voltage in figure 14. As shown in figure 14, the tilt angle dependence on applied voltage does not depend on the liquid crystal layer thickness. This result is similar to that of the threshold voltage of the Freédericksz transition which is independent of the liquid crystal layer thickness.

The reason that the transmittance–voltage curve for the LCPG has maximum and minimum values is attributed to the fact that the electric field in the liquid crystal layer

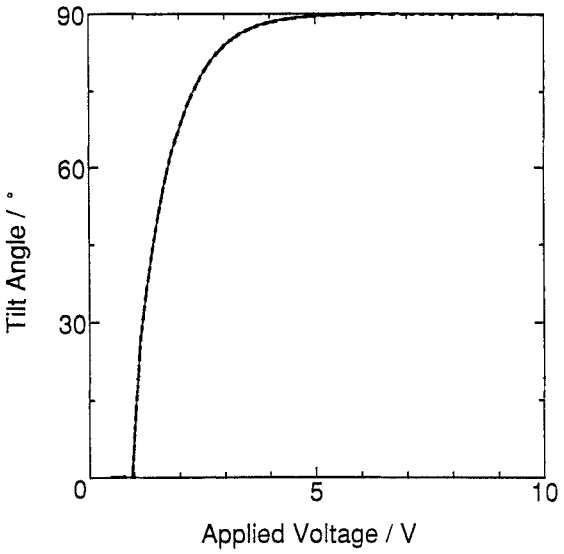

Figure 14. Tilt angle of the molecules in the centre of the liquid crystal layer for different layer thicknesses. The liquid crystal was E7. Layer thicknesses: (- - - -), 1·4 μm; (——), 4·2 μm.

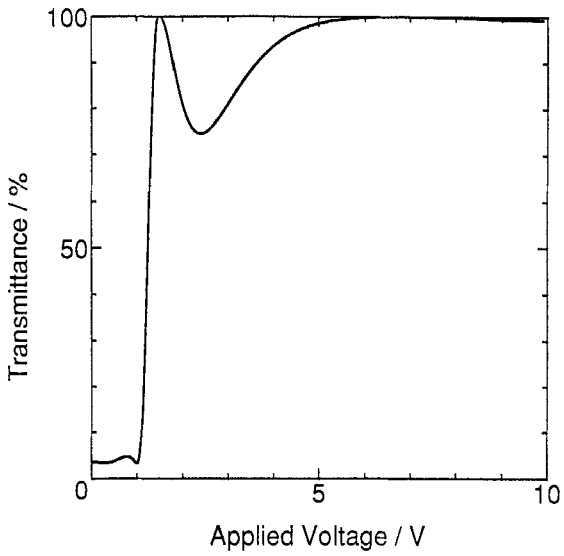

Figure 15. Transmittance–voltage curve simulation for the LCPG which has a gap between the phase grating and the opposite substrate. The grating depth was 1·4 μm, gap 2·8 μm, liquid crystal E7, and wavelength 630 nm.

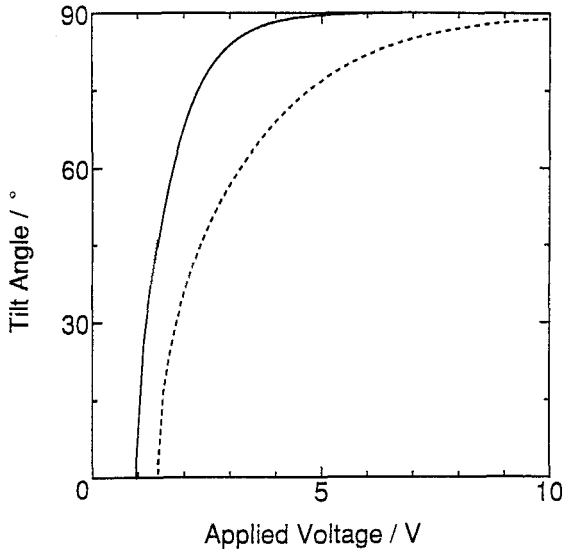

Figure 16. Tilt angle of the molecules in the centre of liquid crystal layer for different thicknesses, when voltage losses for the grating material are considered. (----), plateau part (1·4 μm); (——), groove part (4·2 μm). The liquid crystal was E7.

of the convex part of the grating is less than that of the groove part, because of voltage loss in the grating material. Therefore, the authors assume that applied voltage for the plateau part is given as $(\varepsilon_g/d_g)/(\varepsilon_{LC}/d_{LC}+\varepsilon_g/d_g)$ of the total applied voltage, where ε is the dielectric constant, d is the layer thickness, and subscripts g and LC denote the grating material and liquid crystal, respectively. Under this assumption, the transmittance–voltage curve for the LCPG was calculated and the results are shown in figure 15. The simulated transmittance–voltage curve is closely coincident with the experimental one (figure 7). To consider the liquid crystal situation, the tilt angle of the liquid crystal at the layer centre was also calculated and is shown in figure 16. The response of the liquid crystal in the plateau part is slower than that in the groove part.

Comparison between figures 14 and 16 indicates that the maximum and minimum in transmittance–voltage curve does not appear for the LCPG whose electrode is on the grating surface, because there is no voltage loss caused by the grating part.

As shown previously, the simulation makes it possible to predict LCPG properties from properties of the liquid crystals and the refractive index of a grating material, in spite of the fact that this model ignores the effect of the grating side wall. This method is convenient, because LCPG properties can be predicted from only the properties of the liquid crystal and grating material, without making the LCPGs.

6. Conclusion

Electro-optic properties of the LCPG, regarding groove depth, temperature dependence, and any gap between the grating and an opposite substrate have been studied. Their off response times are proportional to the square of the groove depth. The transmitted light colour and the driving voltage depend on temperature. The transmittance–voltage curve has a maximum and a minimum, when there is a gap between the grating and the opposite substrate. The authors also studied a simulation of these properties, using a homogeneously aligned two part model. The simulation

makes it possible to predict properties of LCPGs from properties of the liquid crystal and the refractive index of the grating material, in spite of this model ignoring the effect of the side walls of the grating groove.

The author would like to thank Ohmiyakasei Chemicals for supplying Elvacite 2041. They are grateful to K. Sumiyoshi and K. Takatori for using the simulator. They are also grateful to H. Kawahara for his kindness in carrying out the deep UV lithography process. They are also grateful to T. Gotoh and G. Saitoh for the valuable advice.

References

[1] KNOP, K., and KANE, J., 1981, U.S. Patent 4,251,137.
[2] MURAI, H., GOTOH, T., SUZUKI, M., HASEGAWA, E., and MIZOGUCHI, K., 1992, *SPIE*, **1665**, 230.
[3] GALE, M. T., KANE, J., and KNOP, K., 1979, *J. appl. Photogr. Engng*, **4**, 41.
[4] Data from a Du Pont catalogue.
[5] Data from BDH and Merck Ltd catalogues.
[6] FUNADA, F., YAMAMOTO, H., and WADA, F., 1973, *Sharp tech. J.*, **12**, 65.
[7] FUNADA, F., KAMIDE, H., WADA, F., and MITO, S., 1975, *Oyo Buturi*, **44**, 866.
[8] GRULER, H., and MEIER, G., 1972, *Molec. Crystals. liq. Crystals.*, **16**, 299.
[9] DEULING, H., 1972, *Molec. Crystals liq. Crystals*, **19**, 123.
[10] BECKER, M., 1989, *Display*, October, p. 215.
[11] WU, C. S., 1986, *J. appl. Phys.*, **60**, 1386.